

## Electronic Supplementary Information

### Peptide-based chemical models for lytic polysaccharide monooxygenases

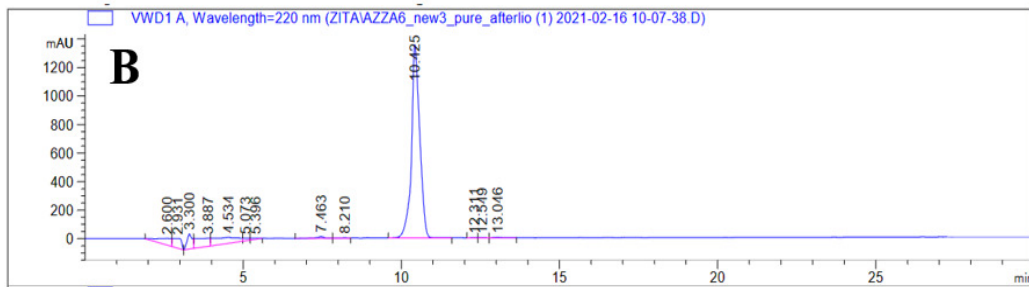
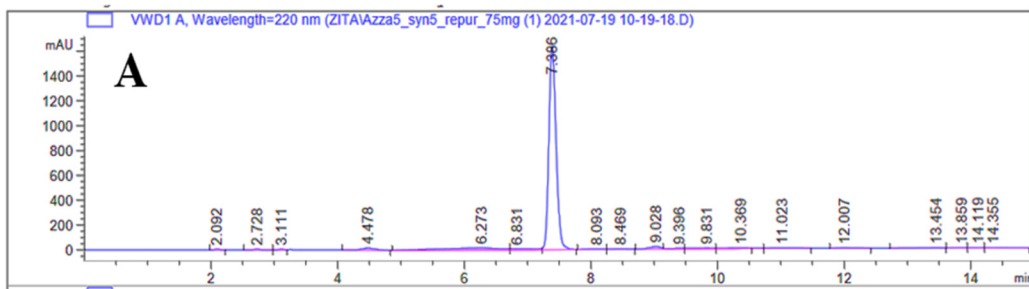
Azza A. Hassoon<sup>a,d</sup>, Attila Szorcsik<sup>a</sup>, Lívía Fülöp<sup>b</sup>, Zita I. Papp<sup>b</sup>, Nóra V. May<sup>c</sup>, Tamás Gajda<sup>a,\*</sup>

<sup>a</sup>*Department of Inorganic and Analytical Chemistry, University of Szeged, Szeged, Hungary*

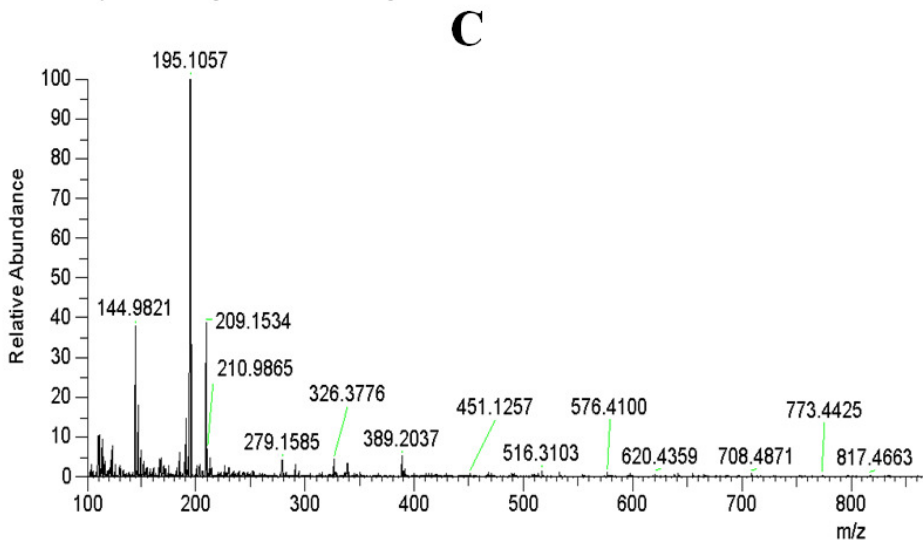
<sup>b</sup>*Institute of Medical Chemistry, University of Szeged, Szeged, Hungary*

<sup>c</sup>*Centre for Structural Science, Research Centre for Natural Sciences, Budapest, Hungary*

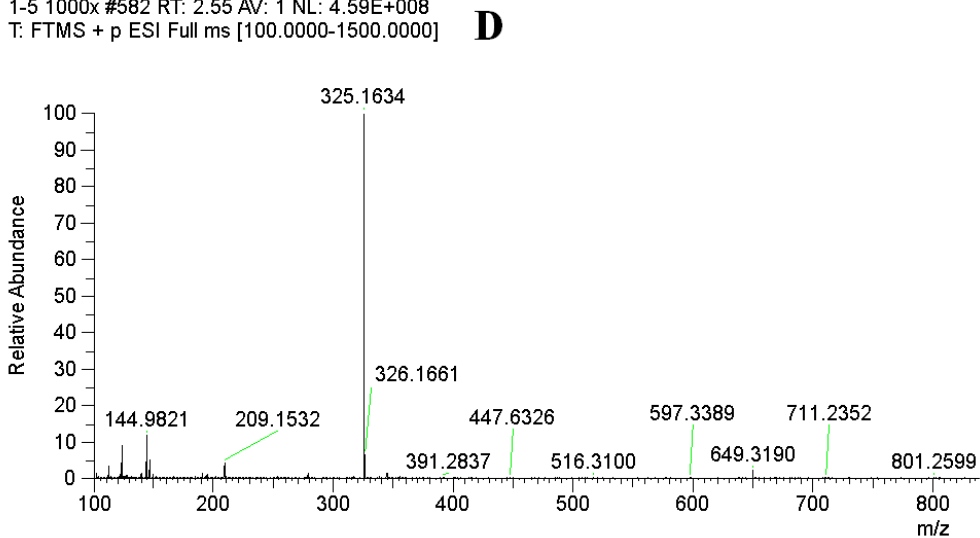
<sup>d</sup>*Chemistry Department, Faculty of Science, Mansoura University, Mansoura, 35516, Egypt*



1-5 1000x #490 RT: 2.15 AV: 1 NL: 1.14E+008  
T: FTMS + p ESI Full ms [100.0000-1500.0000]



1-5 1000x #582 RT: 2.55 AV: 1 NL: 4.59E+008  
T: FTMS + p ESI Full ms [100.0000-1500.0000]



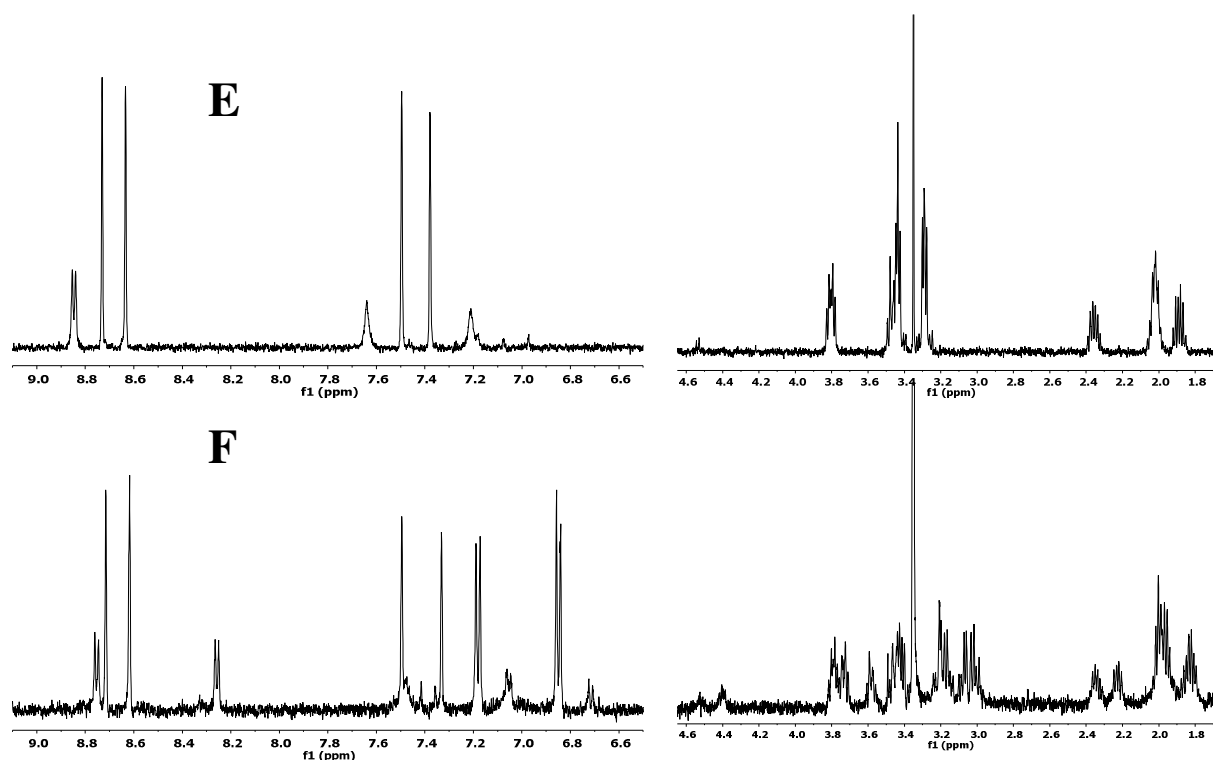


**Figure S1** Analytical HPLC chromatograms (A,B), HR ESI-MS (C,D) and <sup>1</sup>H NMR (E,F) spectra of the purified HPH-NH<sub>2</sub> (**L**<sup>1</sup>) (A,C,E) and HPHPY-NH<sub>2</sub> (**L**<sup>2</sup>) (B,D,F) peptides.

Conditions of HPLC chromatograms: JUPITER C18 column (150 x 4.6 mm, 300 Å pore size, 5 μm particle size), mobile phase A: 0.1% TFA in water, mobile phase B: 0.1% TFA in acetonitrile/water, flow rate: 1.2 ml/min, detection:UV at 220 nm.

HR ESI-MS: (C) *m/z* calc for C<sub>17</sub>H<sub>24</sub>N<sub>8</sub>O<sub>3</sub> [M+H]<sup>+</sup> 389.20, found [M+1]<sup>+</sup> 389.20 (*z* = 1) and [M + 2H]<sup>2+</sup> 195.11 (*z* = 2); (D) *m/z* calc for C<sub>31</sub>H<sub>40</sub>N<sub>10</sub>O<sub>6</sub> [M]<sup>+</sup> 648.31, found [M+1]<sup>+</sup> 649.39 (*z* = 1) and [M + 2H]<sup>2+</sup> 325.16 (*z* = 2). For the assignment of the <sup>1</sup>H NMR peaks see the Experimental part.

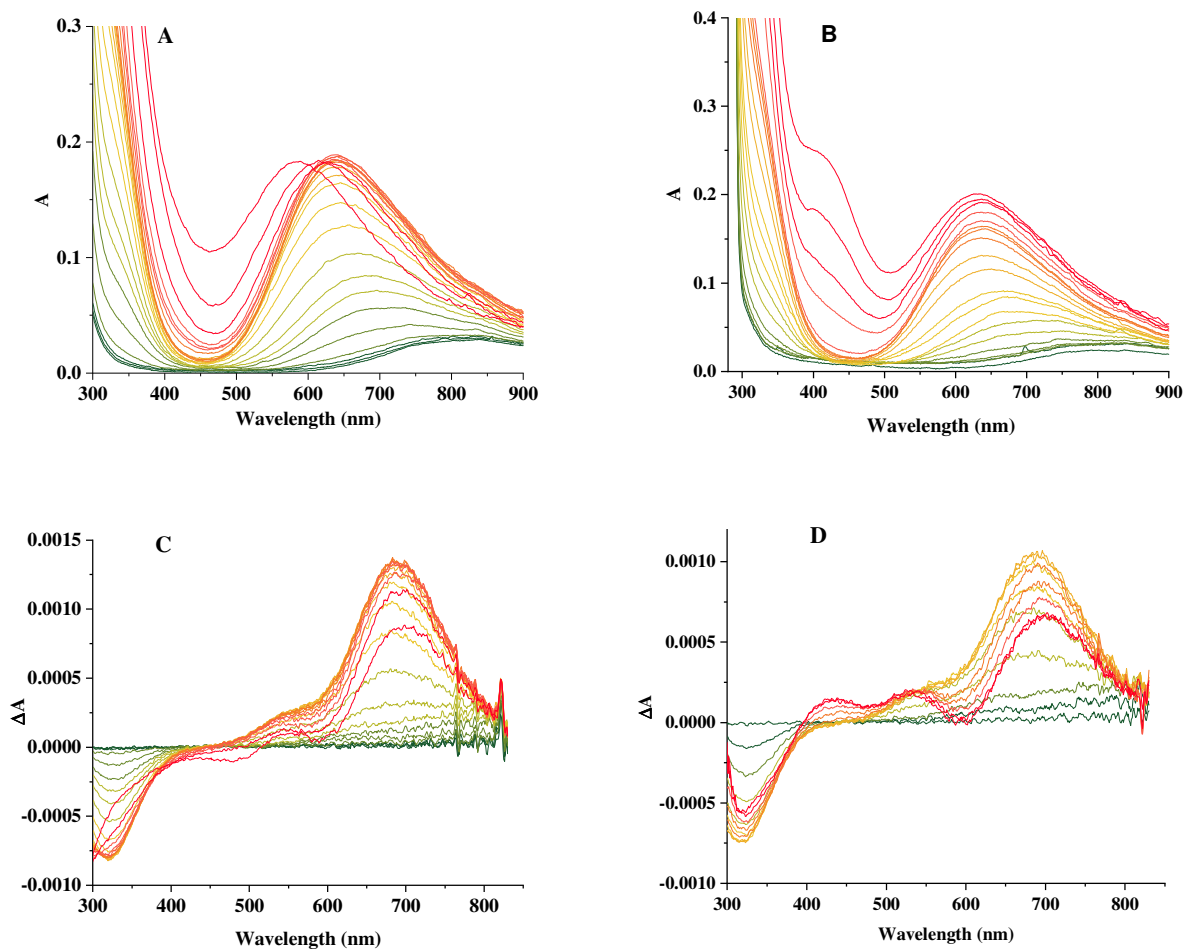


**Figure S2** pH-dependent UV-Vis (A,B) and circular dichroism (C,D) spectra in the Cu(II)-L<sup>1</sup> (A,C) and Cu(II)-L<sup>2</sup> (B,D) systems at 1:2 metal-to-ligand ratios (the pH increases in the green-yellow-red direction,  $T = 298$  K,  $I = 0.2$  M KCl,  $[L]_{\text{tot}} = 0.0014$  M, ).

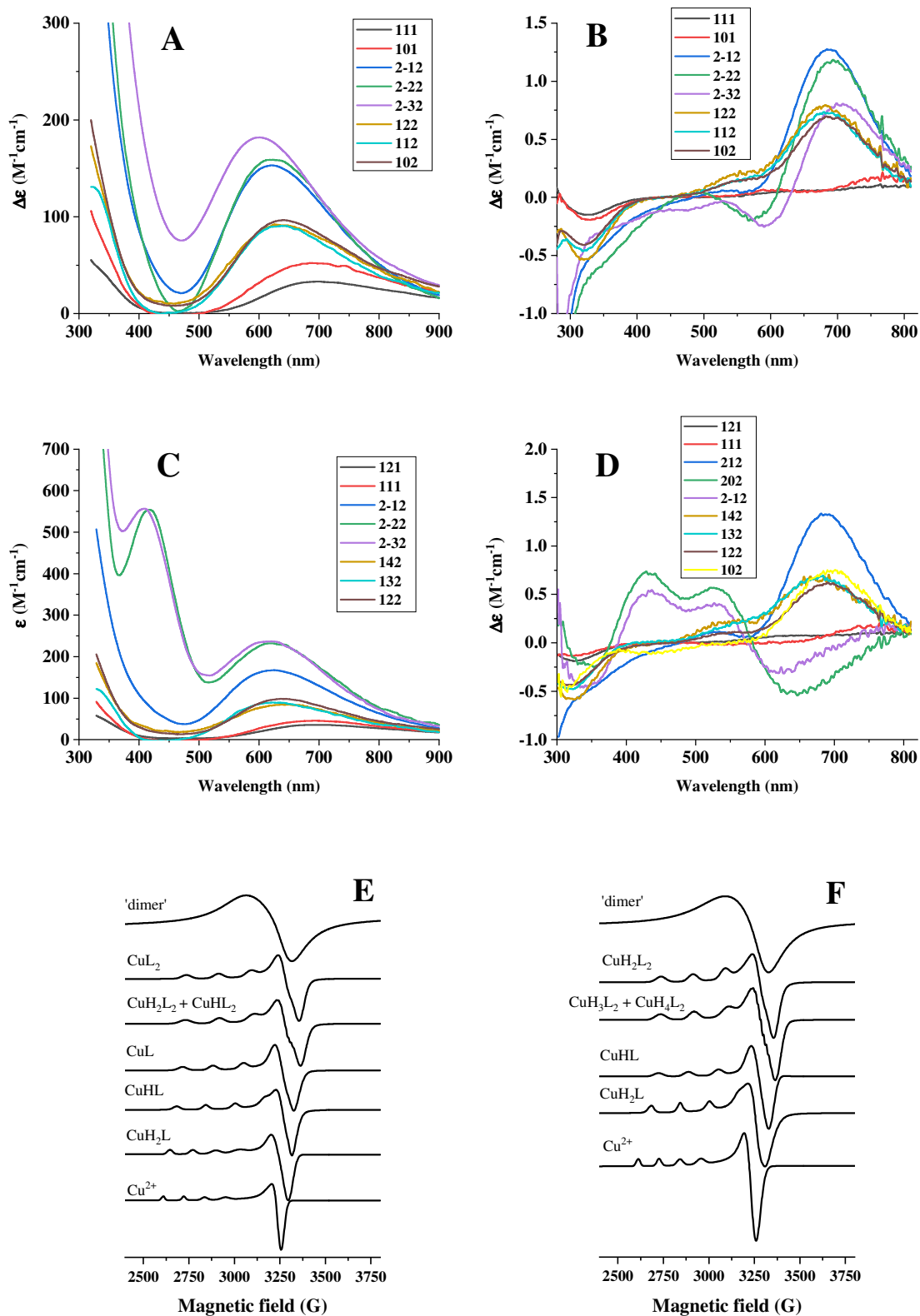


**Figure S3** Individual UV-Vis (A,C), CD (B,D) and EPR (E,F) spectra of the complexes formed in the Cu(II)-L<sup>1</sup> (A,B,E) and Cu(II)-L<sup>2</sup> (C,D,F) systems. UV-Vis and CD spectra were calculated by the computer program PSEQUAD, while the component EPR spectra were obtained using the 'epr' software.

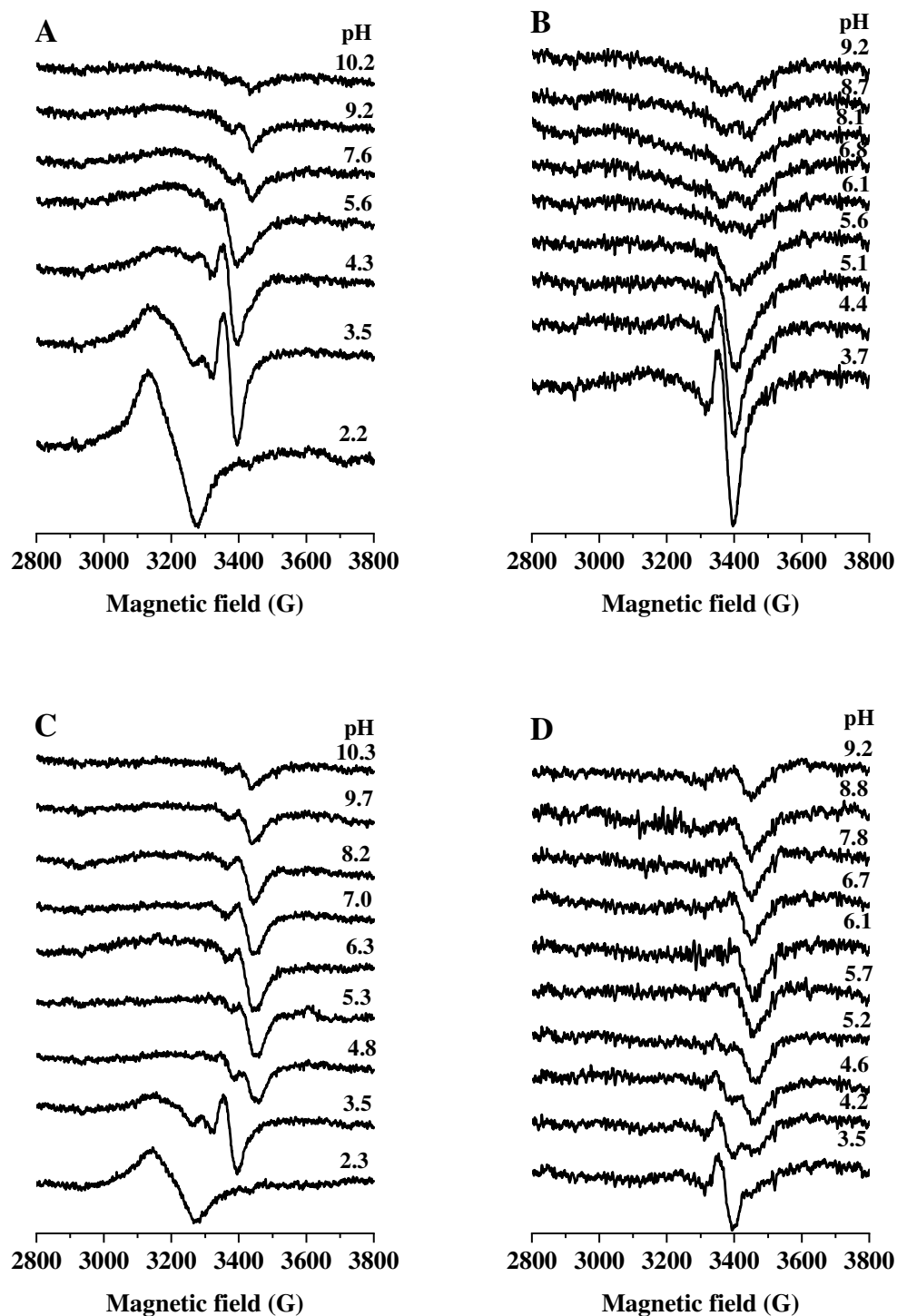


**Figure S4** Experimental X-band CW-EPR spectra recorded at room temperature in the Cu(II)-L<sup>1</sup> (A,C) and Cu(II)-L<sup>2</sup> (B,D) systems at 1:1 (A,B) and 1:2 (C,D) metal-to-ligand ratios (A: [Cu(II)]<sub>tot</sub> = 1.24 mM, [L<sup>1</sup>]<sub>tot</sub> = 1.30 mM, B: [Cu(II)]<sub>tot</sub> = 0.65 mM, [L<sup>2</sup>]<sub>tot</sub> = 1.30 mM, C: [Cu(II)]<sub>tot</sub> = 1.80 mM, [L<sup>1</sup>]<sub>tot</sub> = 1.90 mM, D: [Cu(II)]<sub>tot</sub> = 0.95 mM, [L<sup>2</sup>]<sub>tot</sub> = 1.90 mM)

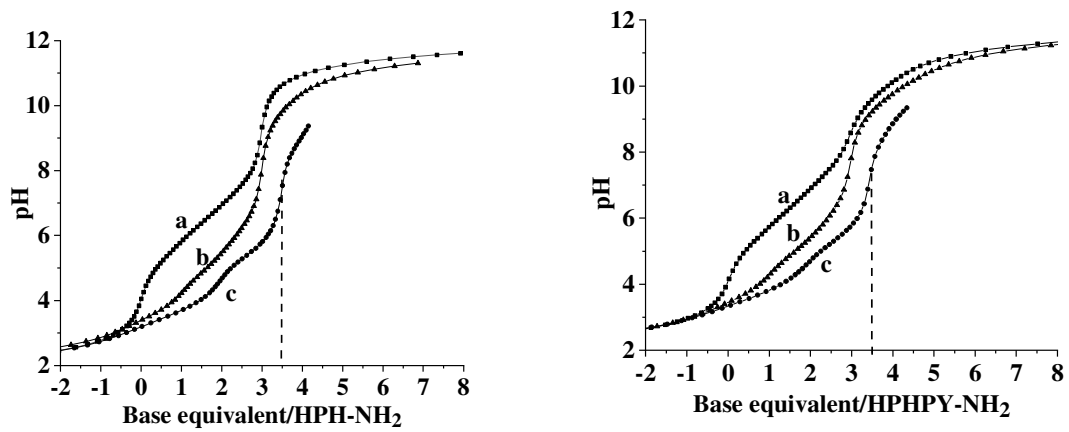


**Figure S5.** Titration curves of the free ligand (a), copper - ligand (II) 1:2 (b) and 1:1 (c) systems as a function of added base equivalent relative to the ligand  $L^1$  (left) and  $L^2$  (right).

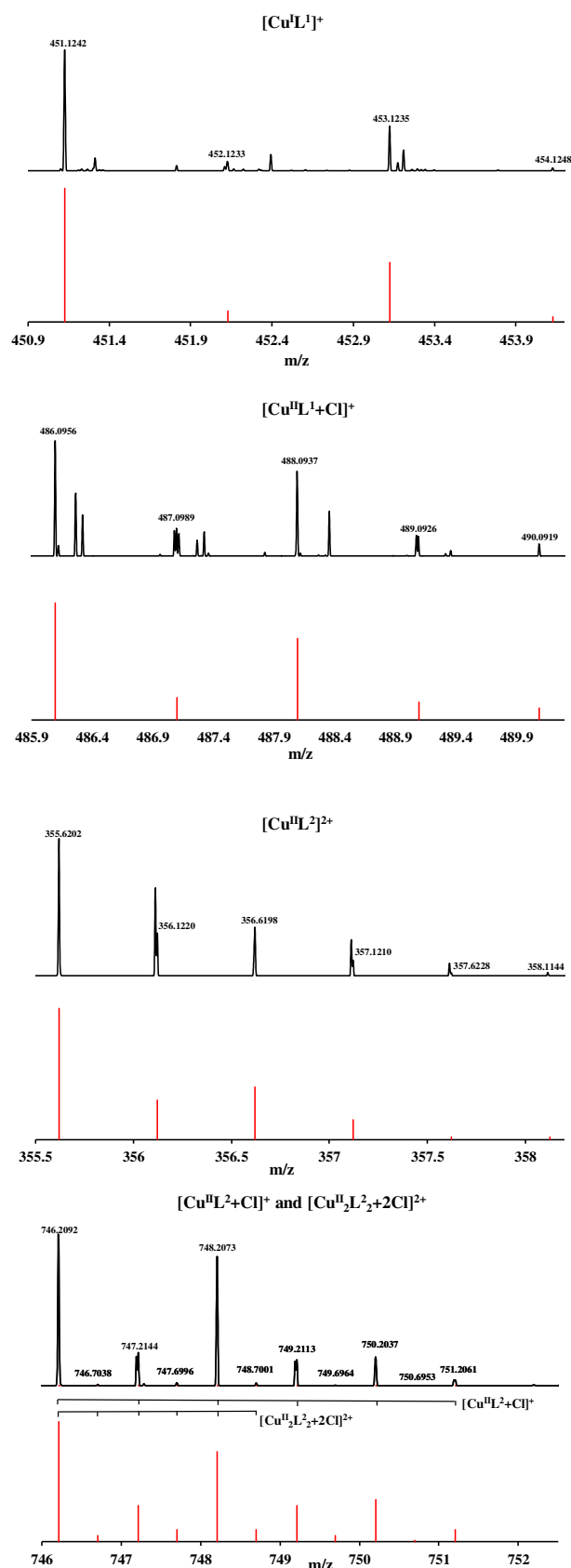


**Figure S6** Monomer and dimer complexes identified on the ESI-MS spectra. The peaks related to the dimer  $[\text{Cu}^{\text{II}}_2\text{L}^2_2+2\text{Cl}]^{2+}$  complex (bottom) have notable lower intensity than those of the monomer species.



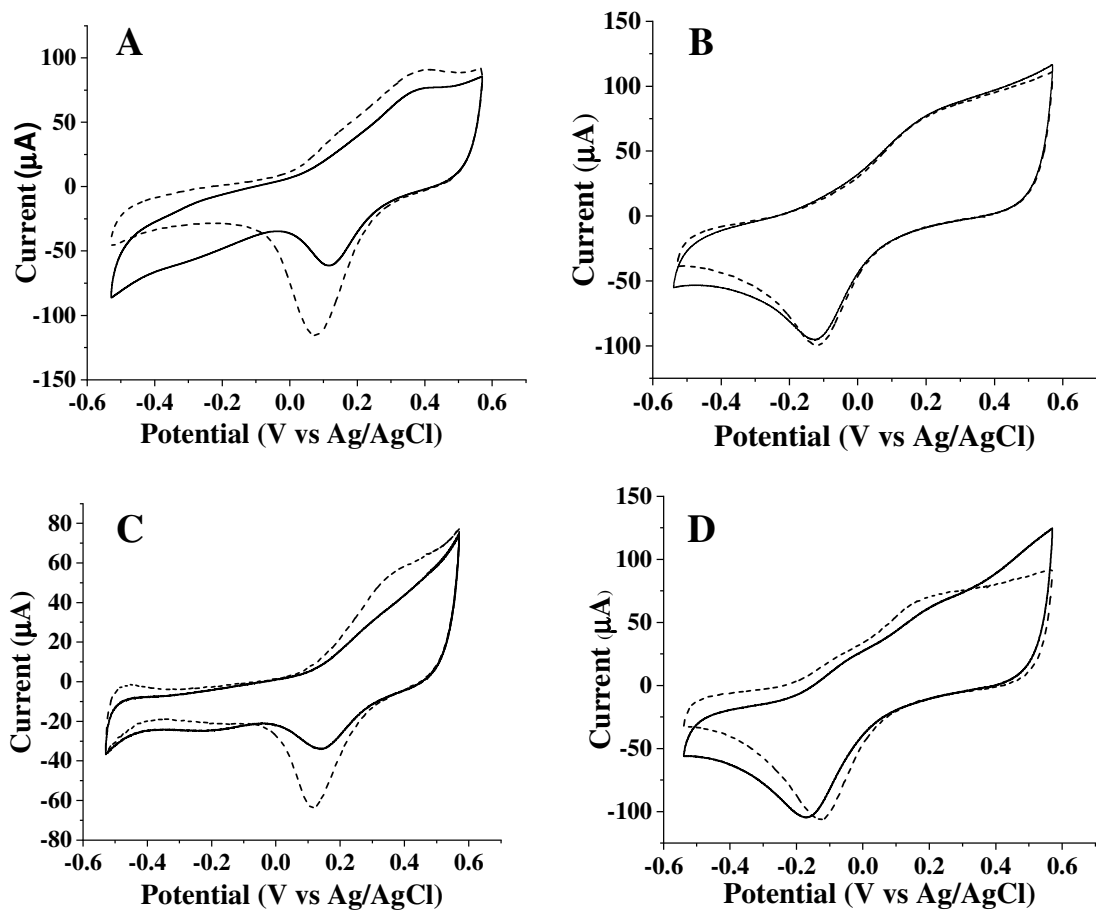


**Figure S7.** Cyclic voltammograms of the Cu(II)-L<sup>1</sup> (A,B) and Cu(II)-L<sup>2</sup> (C,D) 1:1 systems at pH= 7.4 (A,C) and pH = 10.5 (B,D) in absence (continuous lines) and in presence (dashed lines) of 1.1 equivalent H<sub>2</sub>O<sub>2</sub> ( $T = 298$  K,  $I = 0.2$  M KCl,  $[L]_{\text{tot}} = 0.6$  mM).

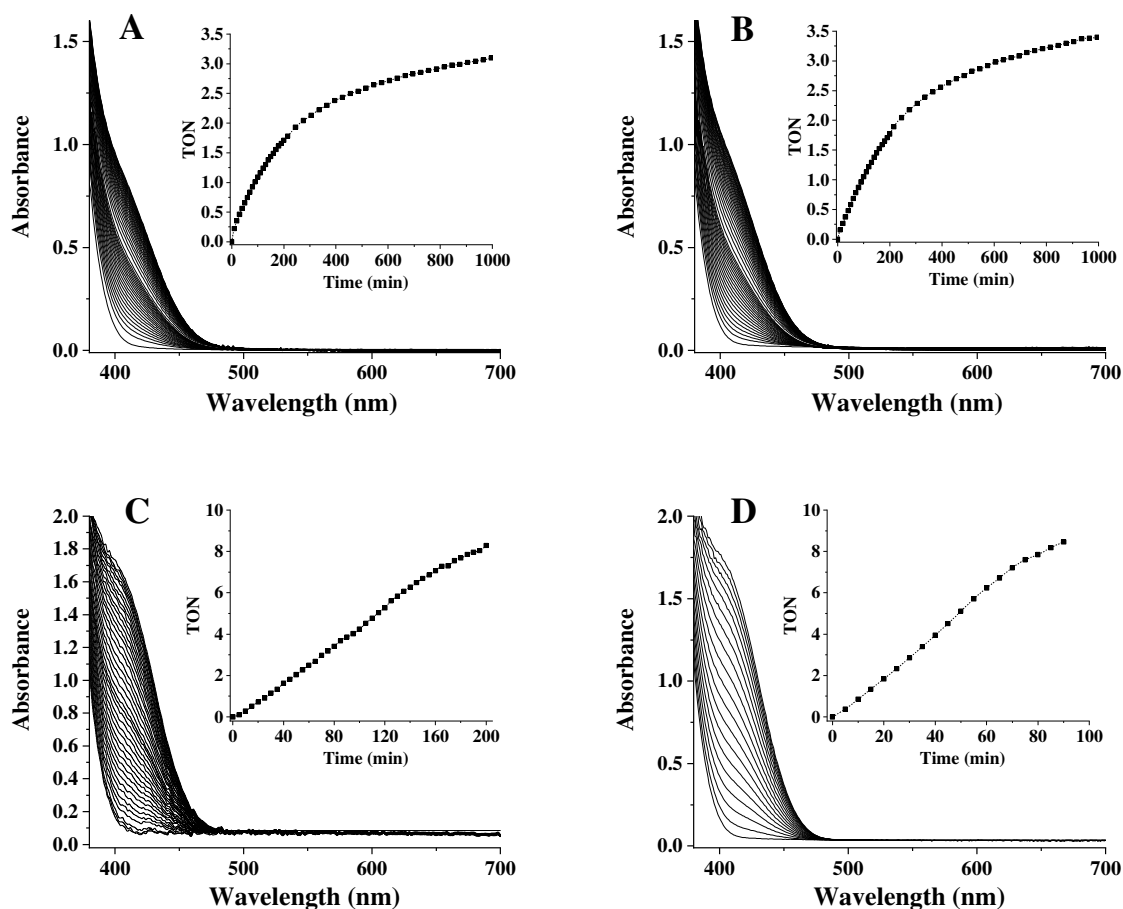


**Figure S8** Time-dependent formation of *p*-nitrophenolate during the oxidation of PNPG catalysed by the Cu(II)-L<sup>1</sup> (A,C) and Cu(II)-L<sup>2</sup> (B,D) 1:1 systems at pH 7.4 (A,B) and pH 10.5 (C,D); the inserts show the plot of turnover number (TON) as a function of time. (At pH = 7.4: [H<sub>2</sub>O<sub>2</sub>] = [PNPG] = 20 mM, [Cu(II)]<sub>tot</sub> = 0.1 mM, 5 mm cuvette; at pH = 10.5 [H<sub>2</sub>O<sub>2</sub>] = 10 mM, [PNPG] = 5 mM, [Cu(II)]<sub>tot</sub> = 0.01 mM, 10 mm cuvette).

The reason of saturation behaviour at pH 7.4 is unknown, but maybe related to the oxidation of the peptides during such long-term kinetic studies.

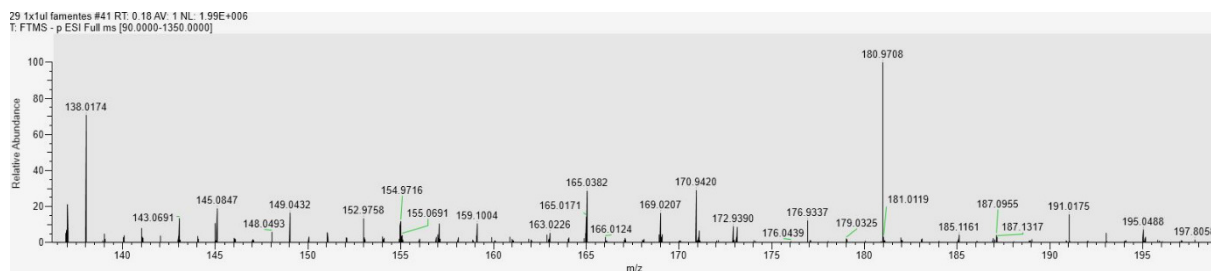


**Figure S9** ESI-MS spectrum in negative mode of the reaction mixture of PNPG oxidation promoted by the Cu(II)-L<sup>1</sup> system after 4h reaction time (pH = 10.5 [H<sub>2</sub>O<sub>2</sub>] = 10 mM, [PNPG] = 1 mM, [Cu(II)]<sub>tot</sub> = 0.05 mM). The peaks at m/z = 138.0174 and 195.0488 corresponds to *p*-nitrophenolate (calc. m/z = 138.0191) and gluconate (calc. m/z = 195.0505) anions, respectively.

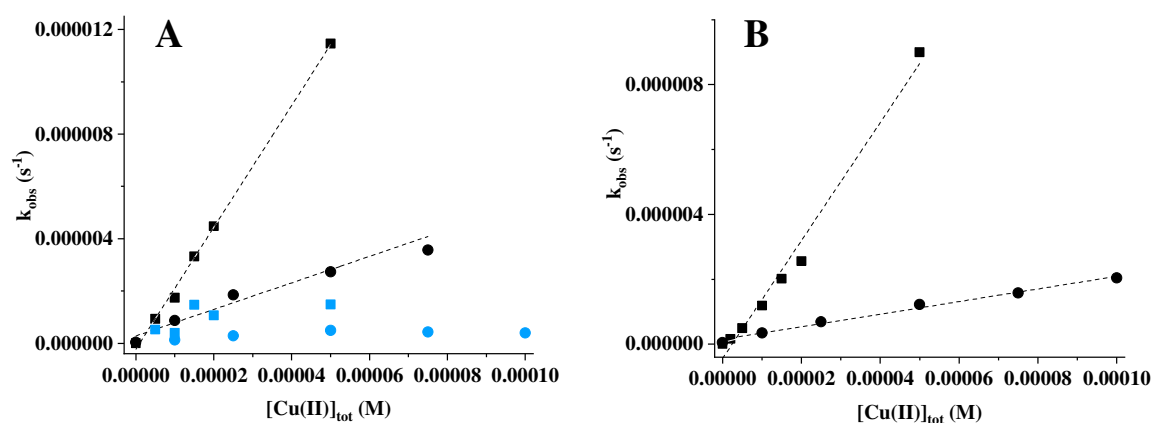


**Figure S10** Dependence of  $k_{\text{obs}}$  of PNPG oxidation on the copper(II) concentration in the Cu(II)-L<sup>1</sup> (A) and Cu(II)-L<sup>2</sup> (B) 1:1 systems at pH = 7.4 (●) and 10.5 (■); [PNPG] = [H<sub>2</sub>O<sub>2</sub>] = 10 mM. Blue signs in figure A show the effect of CuCl<sub>2</sub> concentration, in the absence of peptides.

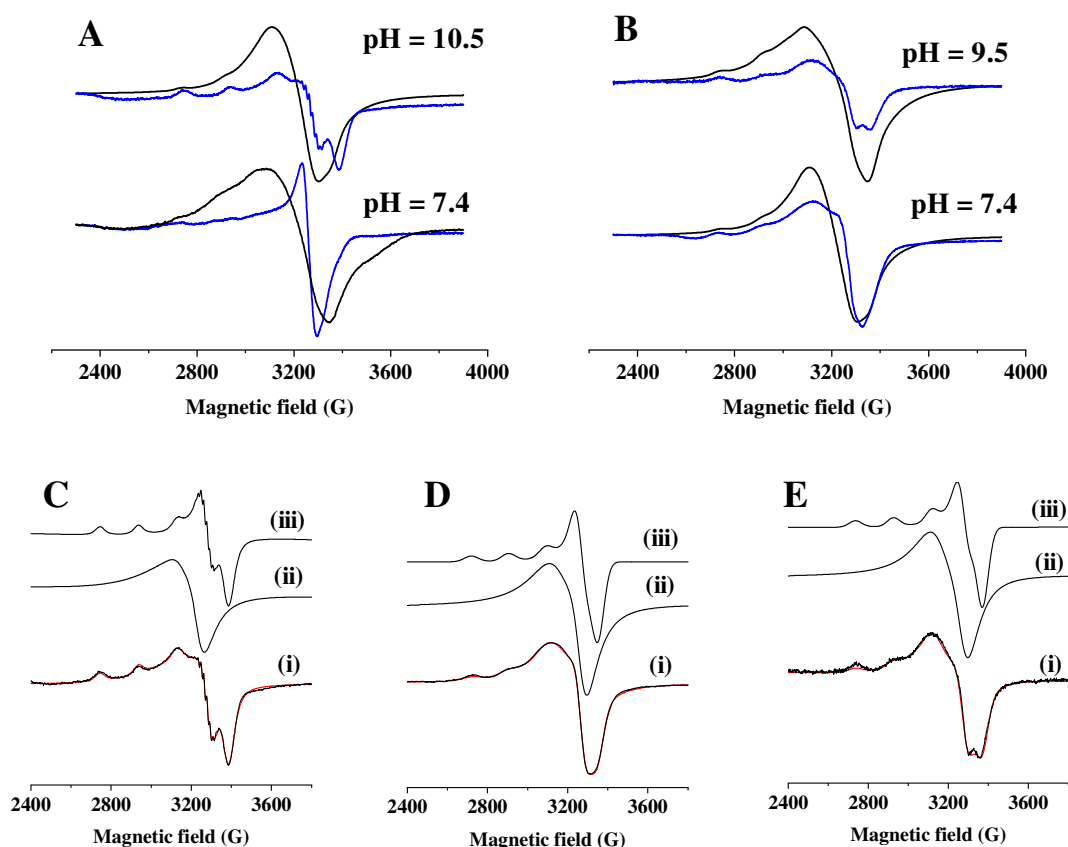


**Figure S11.** A,B: The change of 77K EPR spectra upon addition of 25 eq. H<sub>2</sub>O<sub>2</sub> in the Cu(II)-L<sup>1</sup> (A) and Cu(II)-L<sup>2</sup> (B) 1:1 systems. C,D,E: Deconvolution of the EPR spectra obtained after addition of H<sub>2</sub>O<sub>2</sub> to the (C) Cu(II)-L<sup>1</sup> at pH 10.5, (D) Cu(II)-L<sup>2</sup> at pH 7.4, (E) Cu(II)-L<sup>2</sup> at pH 9.5; (i) experimental (black) and simulated (red) spectra, (ii) and (iii) are the component spectra of the dimer and monomer complexes, respectively.

The EPR parameters of the mononuclear (hydro)peroxo complexes: (C)  $g_{\perp} = 2.045(2)$ ,  $g_{\parallel} = 2.222(2)$ ,  $A_{\perp} = 14(2)$  G,  $A_{\parallel z} = 189(2)$  G,  $A_{N,\perp} = 15(2)$  G; (D)  $g_{\perp} = 2.058(2)$ ,  $g_{\parallel} = 2.248(2)$ ,  $A_{\perp} = 12(5)$  G,  $A_{\parallel} = 182(2)$  G; (E)  $g_{\perp} = 2.050(2)$ ,  $g_{\parallel} = 2.231(2)$ ,  $A_{\perp} = 10(5)$  G,  $A_{\parallel} = 186(2)$  G. Isotropic components were described with singlet lines.

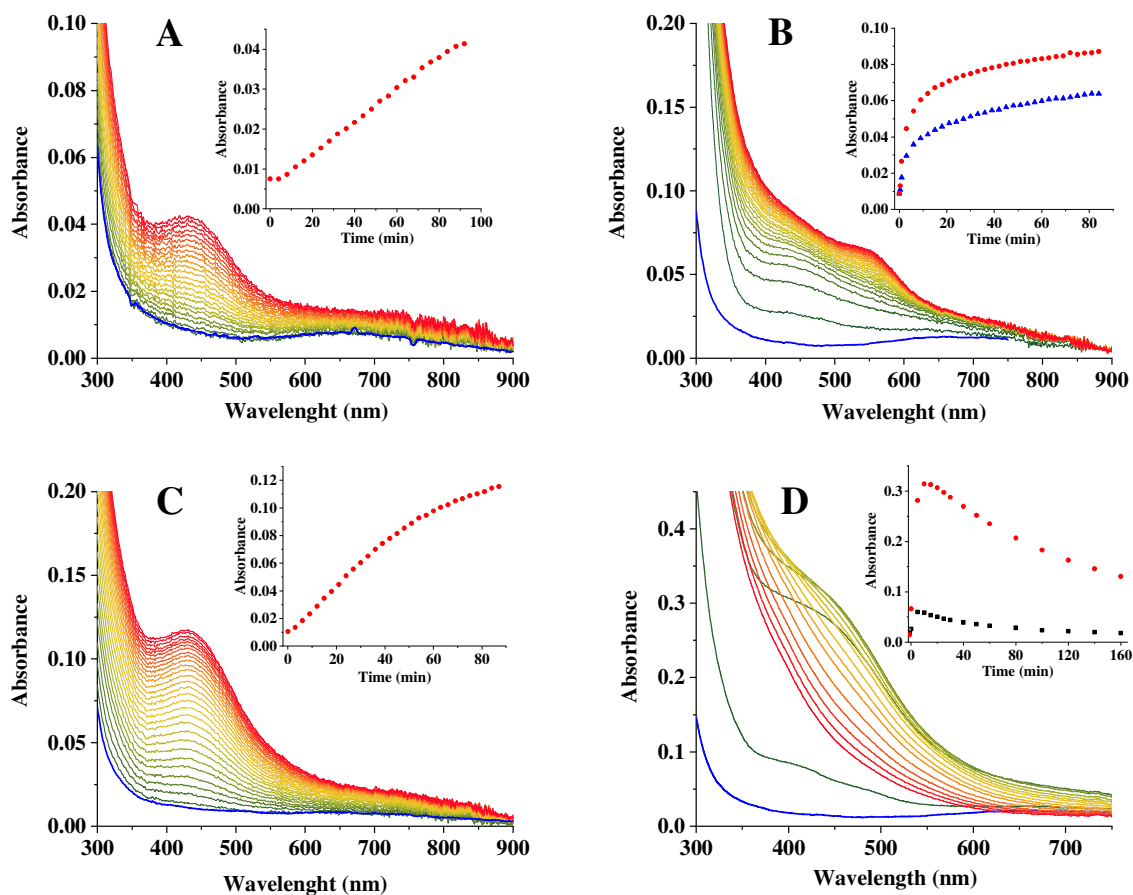


**Figure S12** Time dependence of UV-Vis spectra of the Cu(II)-L<sup>2</sup> 1:1 systems upon addition of 1.1 eq. (A,B) 10 eq. (C) and 200 eq. H<sub>2</sub>O<sub>2</sub> (D) at pH 7.4 (A,C,D) and at 10.5 (B). Blue lines: the initial spectra, green-to-yellow-to-red lines changes upon addition of H<sub>2</sub>O<sub>2</sub>. Inserts show the time dependence of spectrum intensity at 440 nm (●), 550 nm (▲) and 650 nm (■). ([Cu(II)] = 0.05 mM, 20 mm cuvette (A,B,C) and 50 mm cuvette (D));

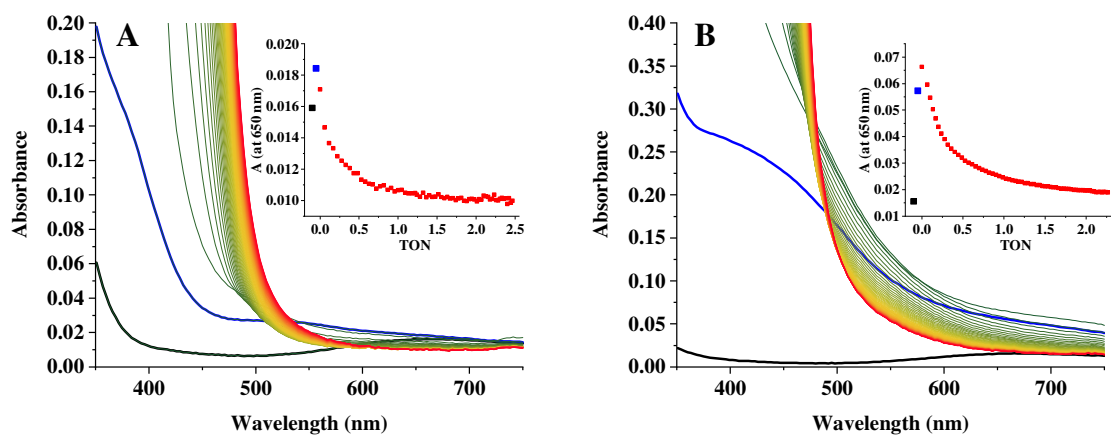
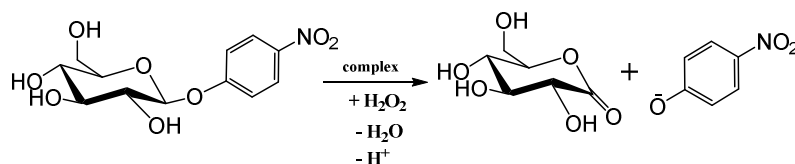


**Figure S13** UV-Vis spectra of the Cu(II)-L<sup>1</sup> (A) and Cu(II)-L<sup>2</sup> (B) 1:1 systems at pH 7.4 and at [Cu(II)] = [HPH] = 0.05 mM in 50 mm cuvette (black line), + 10 mM H<sub>2</sub>O<sub>2</sub> (blue line), + 10 mM PNPG time dependence up to 650 minutes (green-to-red lines); insert show the change of spectrum intensity at 650 nm as a function of turn-over number (TON); initial spectrum (■), + 10 mM H<sub>2</sub>O<sub>2</sub> (■), time (TON) dependent changes after addition of 10 mM PNPG (■). TONs were calculated based on the absorbances at 450 nm where  $\epsilon_{\text{p-nitrophenolate}}(450\text{nm}) \sim 0.2 * \epsilon_{\text{p-nitrophenolate}}(400\text{nm})$ .



**Scheme S1:** Scheme for the oxidative conversion of p-nitrophenyl- $\beta$ -D-glucopyranoside

**Table S1** Cathodic and anodic peaks observed by cyclic voltammetry in the Cu(II)-L<sup>1</sup> and Cu(II)-L<sup>2</sup> 1:1 systems ([Cu(II)]<sub>tot</sub> = 0.6 mM, [H<sub>2</sub>O<sub>2</sub>] = 0.66 mM, [buffer] = 0.1 M, I = 0.2 M KCl). Potentials are given in V vs. Ag/AgCl electrode.

peptide	pH	1.1 eq. H <sub>2</sub> O <sub>2</sub>	Ep <sup>c</sup> (V)	Ep <sup>mi*</sup> (V)	Ep <sup>ma**</sup> (V)
<b>L<sup>1</sup></b>	7.4	-	0.11	~ 0.16	0.39
		+	0.07	~ 0.16	0.40
	10.5	-	-0.13	-	0.21
		+	-0.12	-	0.21
<b>L<sup>2</sup></b>	7.4	-	0.14	-	0.31
		+	0.11	-	0.35
	10.5	-	-0.18	~ -0.03	0.19
		+	-0.13	~ -0.07	0.17

\*minor anodic peak

\*\* major anodic peak